$\pi^- p$ Interactions at 10 GeV/c with Four Charged Secondaries

N. N. Biswas, I. Derado,* N. Schmitz, and W. D. Shephard*†
Max-Planck-Institut für Physik und Astrophysik, München, Germany
(Received 9 January 1964)

About 800 $\pi^- p$ interactions with four charged secondaries produced by 10.25-GeV/c negative pions in the 81-cm Saclay hydrogen bubble chamber have been analyzed. The cross sections for the various reactions, including the production of N^*, ρ, and ω are given in Tables I and III. The c.m.-system angular and momentum distributions are discussed; the nucleons are strongly peaked backward whereas the pions, especially the π^-, go predominantly forward. Values for the average transverse momentum of the various secondary particles have been determined. From plots of the average transverse momentum versus the c.m.-system longitudinal momentum correlations between the momentum p^* and the scattering angle Θ^* can be seen; it is found that p^* is essentially proportional to the inverse of $\sin\Theta^*$. The occurrence of resonant states has been investigated. Production of ρ^0 seems very important at this energy in the $p\pi^-\pi^+\pi^-$ final state. Production of N^{*++} is relatively more important in final states involving additional pions and a proton.

1. INTRODUCTION

We have analyzed about 800 interactions with four charged secondaries produced by 10.25-GeV/c negative pions in the 81-cm Saclay hydrogen bubble chamber with a magnetic field of 20.7 kG at the center. In the same films other event types have been studied by the following groups: two-prong events by Fleury *et al.*,[1] elastic scatterings by Brandt *et al.*,[2] six- and eight-prong events by Bardadin *et al.*,[3] and strange-particle productions by Bigi *et al.*[4] More details about the π^- beam can be found in these references. The reactions involved in the present study are:

$$\pi^- p \rightarrow p\pi^-\pi^+\pi^- \quad (1)$$
$$\rightarrow p\pi^-\pi^+\pi^-\pi^0 \quad (2a)$$
$$\rightarrow n\pi^-\pi^+\pi^-\pi^+ \quad (2b)$$
$$\rightarrow p\pi^-\pi^+\pi^-(m\pi^0), \quad m\geqslant 2 \quad (3a)$$
$$\rightarrow n\pi^-\pi^+\pi^-\pi^+(m\pi^0), \quad m\geqslant 1. \quad (3b)$$

2. EXPERIMENTAL DETAILS AND CROSS SECTIONS

The primary π^- beam with an average momentum of 10.25 GeV/c had a rather large momentum spread of ± 0.7 GeV/c. This spread makes event identification rather difficult since it increases the number of kinematically acceptable reaction hypotheses. Nevertheless we have applied the usual procedure of analysis to our events. Only those events which occurred in a limited fiducial volume of the chamber were chosen in order to assure a minimum track length of at least 20 cm for secondaries going in the forward direction. The track measurements were first processed by a geometric reconstruction program and then by a kinematic fitting program on the electronic computer G3 of the Max-Planck-Institut für Physik und Astrophysik. The kinematic fitting and the measurement or visual estimate of the bubble density on positive tracks with a momentum less than $\sim$1.5 GeV/c enabled us to identify about 70% of all events uniquely. For the large majority of the 30% ambiguous events only two hypotheses were acceptable. Each such ambiguous event has been split with proper weighting factors among the possible hypotheses. Most ambiguities, of course, arose between the two reactions (3a) and (3b) for which no fit can be carried out so that one can distinguish between them only by ionization. The various distributions shown and discussed in the next sections were plotted separately for the uniquely identified and for the split-ambiguous events in order to make sure that the results were not influenced by the ambiguities. Each pair of corresponding distributions looked very similar; when there was a difference between a distribution for well identified events and the corresponding distribution for split events this difference was expected and easily explainable. For instance, the c.m.-system proton angular distribution for reactions

TABLE I. Numbers of events and cross sections.

Channel	Number of unambiguous events plus contribution from ambiguous events	Cross section in mb
$p\pi^-\pi^+\pi^-$	76+16.2= 92.2	1.01±0.21
$p\pi^-\pi^+\pi^-\pi^0$	124+37.5=161.5	1.77±0.35
$n\pi^-\pi^+\pi^-\pi^+$	71+23.3= 94.3	1.03±0.24
$p\pi^-\pi^+\pi^-(m\pi^0)$	130+73 =203	2.22±0.56
$n\pi^-\pi^+\pi^-\pi^+(m\pi^0)$	137+73 =210	2.30±0.56
Total	761	8.33±0.35

* Permanent address: Physics Department, University of Notre Dame, Notre Dame, Indiana.
† Fulbright Senior Research Scholar, 1962–63.

[1] P. Fleury, G. Kayas, F. Muller, and C. Pelletier, *Proceedings of the 1962 International Conference on High-Energy Physics at CERN*, edited by J. Prentki (CERN, Geneva, 1962), p. 597.

[2] S. Brandt, V. T. Cocconi, D. R. O. Morrison, A. Wroblewski, P. Fleury, G. Kayas, F. Muller, and C. Pelletier, Phys. Rev. Letters **10**, 413 (1963).

[3] M. Bardadin, L. Michejda, S. Otwinowski, and R. Sosnowski, Proceedings of the Siena International Conference on Elementary Particles (to be published).

[4] A. Bigi, S. Brandt, R. Carrara, W. A. Cooper, A. de Marco, *et al.*, *Proceedings of the 1962 International Conference on High-Energy Physics at CERN*, edited by J. Prentki (CERN, Geneva, 1962), p. 247.

(2a) and (3a) turned out to be peaked backward more strongly for the identified events than for the ambiguous events; this is expected since a proton going backward in the c.m. system usually has a small momentum in the lab system and can thereby be identified. On the other hand a proton which does not go approximately in the backward direction has a higher lab momentum which may make the event identification impossible. In the angular, momentum, and effective-mass distributions presented in this paper the contributions from the uniquely identified events are indicated by the dotted histograms.

In order to check the reproducibility of the measurements and of the event identification a large group of

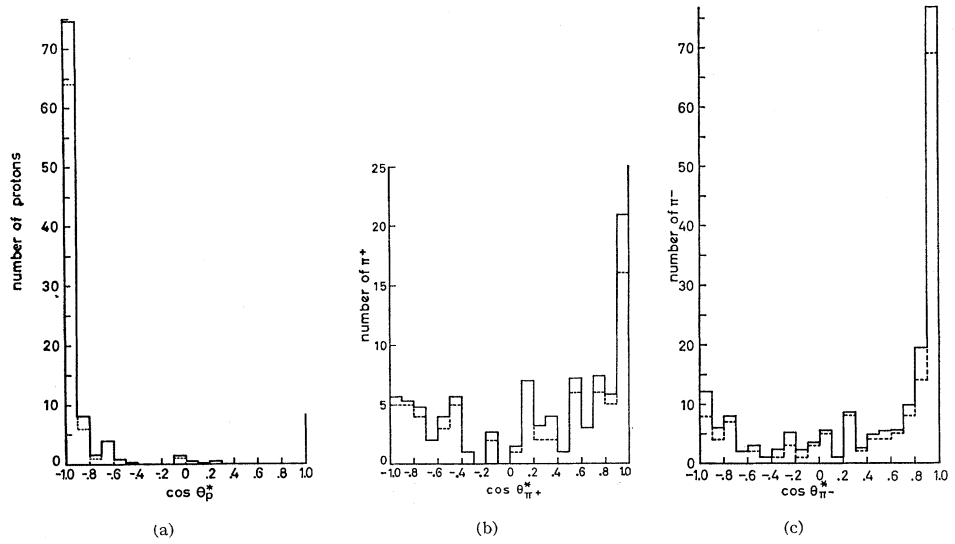

FIG. 1. C.m.-system angular distributions for reaction $\pi^- p \to p\pi^-\pi^+\pi^-$; (a) proton, (b) π^+, (c) π^-.

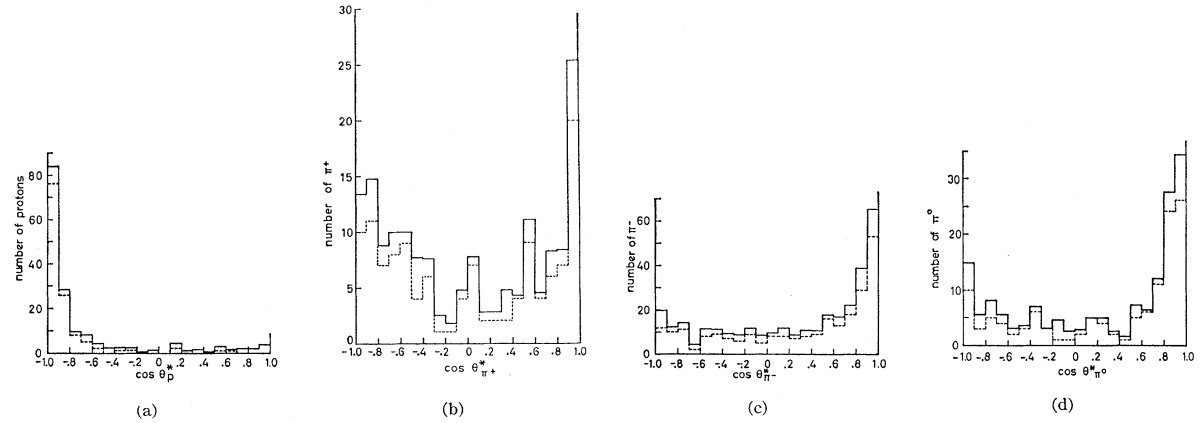

FIG. 2. C.m.-system angular distributions for reaction $\pi^- p \to p\pi^-\pi^+\pi^-\pi^0$; (a) proton, (b) π^+, (c) π^-, (d) π^0.

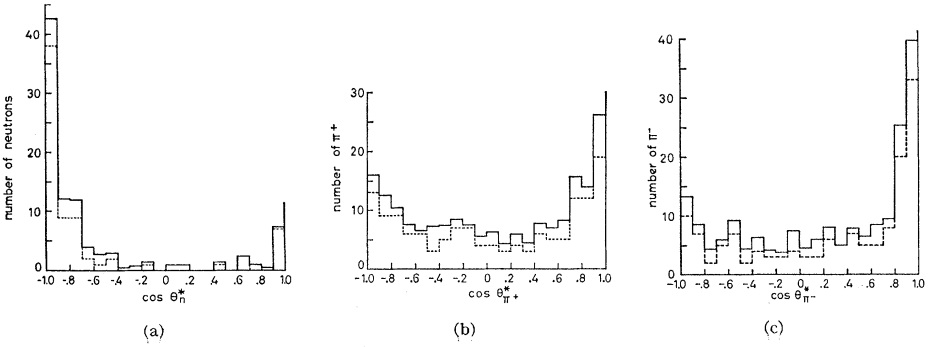

FIG. 3. C.m.-system angular distributions for reaction $\pi^- p \to n\pi^-\pi^+\pi^-\pi^+$; (a) neutron, (b) π^+, (c) π^-.

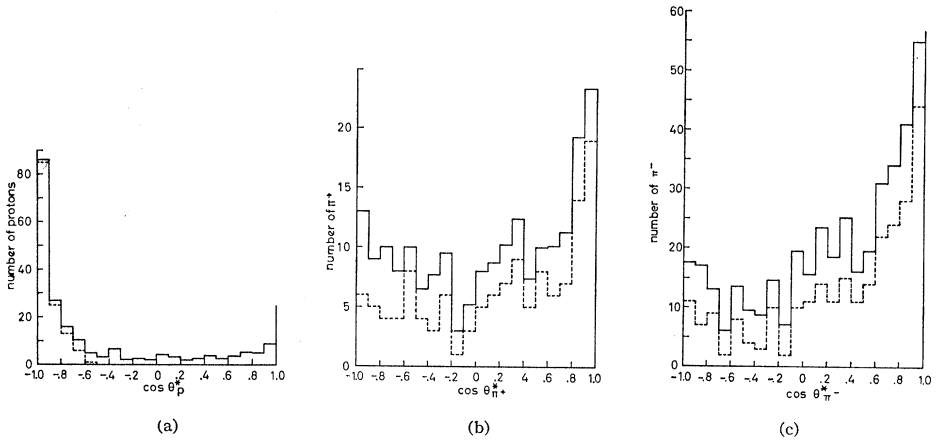

FIG. 4. C.m.-system angular distributions for reaction $\pi^- p \to p\pi^-\pi^+\pi^-(m\pi^0)$; (a) proton, (b) π^+, (c) π^-.

events has been measured twice. In practically all cases the second measurement led to the same result as the first one.

The distributions of missing-mass squared for different event groups were examined as a check on the classification of events. The distributions exhibit effects which are consistent with the large uncertainty in primary momentum. The distribution for reaction (1) is consistent with a fairly pure sample of events. In the case of reactions (2a) and (2b) the distributions are broader and less symmetric about the expected values. The deviations from symmetry are greatest for reaction (2b). Although there is perhaps some contamination of events with more than one neutral secondary in these categories we believe that our conclusions are not qualitatively affected.

In Table I the number of uniquely identified events, the assigned contribution from the ambiguous events, and the cross section are given for each of the five channels (1) to (3b). A beam contamination of 10% muons[2] has been taken into account. A hydrogen density of 0.0625 g cm^{-3} was used. The errors quoted include the statistical errors and the ambiguities in identification. The total cross section of (8.33±0.35) mb for four-prong events without strange particles is to be compared with a value of (10.5±0.3) mb found by the Paris Group[1] which includes also strange-particle production.

3. ANGULAR AND MOMENTUM DISTRIBUTIONS

Figures 1–5 show the c.m.-system angular distributions for the various secondary particles involved in the five reactions (1) to (3b). The dotted histograms represent the distributions obtained from only the unambiguous events. In every case the nucleon distribution is peaked very strongly backward. The π^- go

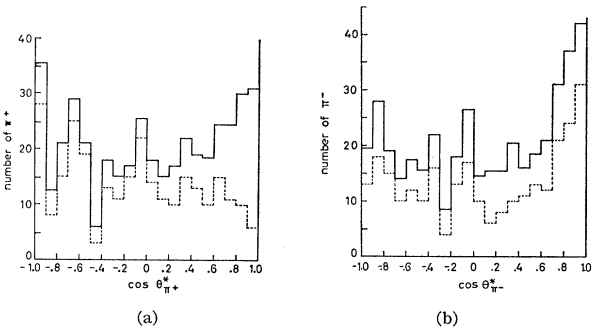

FIG. 5. C.m.-system angular distributions for reaction $\pi^- p \to n\pi^-\pi^+\pi^-\pi^+(m\pi^0)$; (a) π^+, (b) π^-.

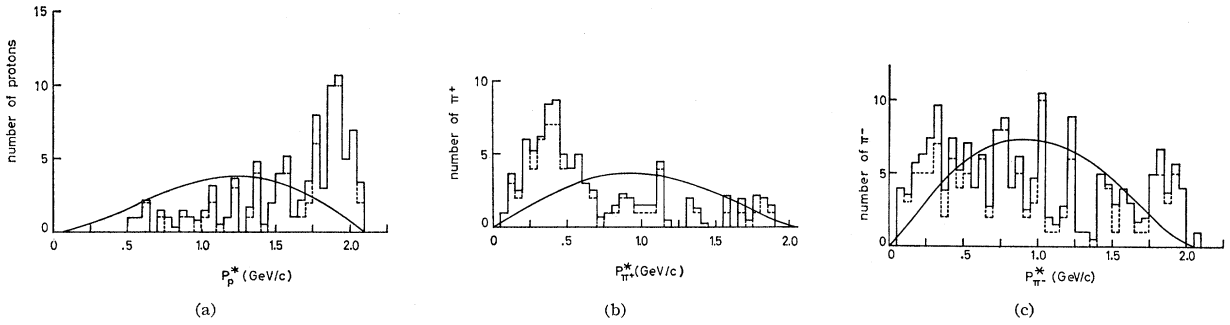

FIG. 6. C.m.-system momentum distributions for reaction $\pi^- p \to p\pi^-\pi^+\pi^-$; (a) proton, (b) π^+, (c) π^-.

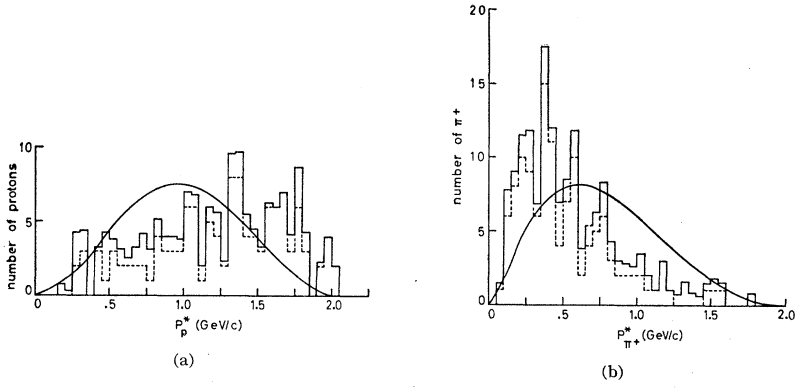

FIG. 7. C.m.-system momentum distributions for reaction $\pi^- p \rightarrow p\pi^-\pi^+\pi^-\pi^0$; (a) proton, (b) π^+, (c) π^-, (d) π^0.

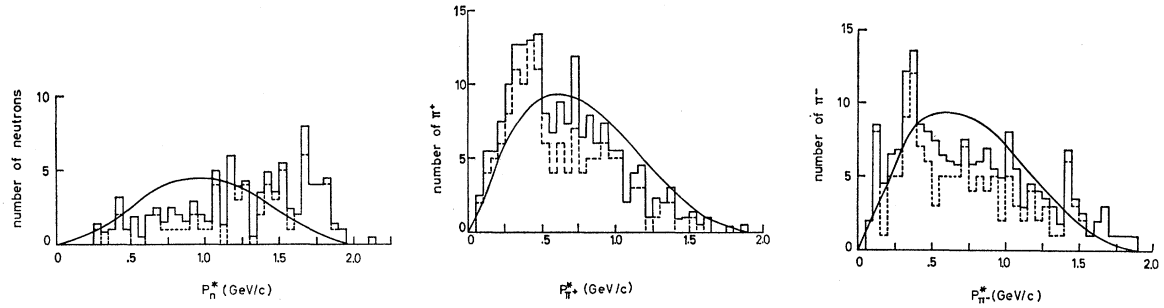

FIG. 8. C.m.-system momentum distributions for reaction $\pi^- p \rightarrow n\pi^-\pi^+\pi^-\pi^+$; (a) neutron, (b) π^+, (c) π^-.

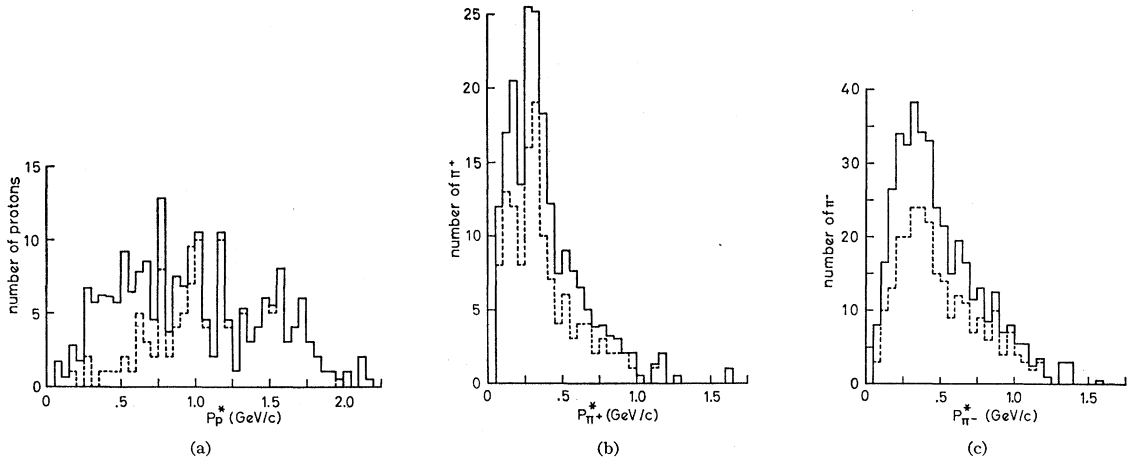

FIG. 9. C.m.-system momentum distributions for reaction $\pi^- p \rightarrow p\pi^-\pi^+\pi^-(m\pi^0)$; (a) proton, (b) π^+, (c) π^-.

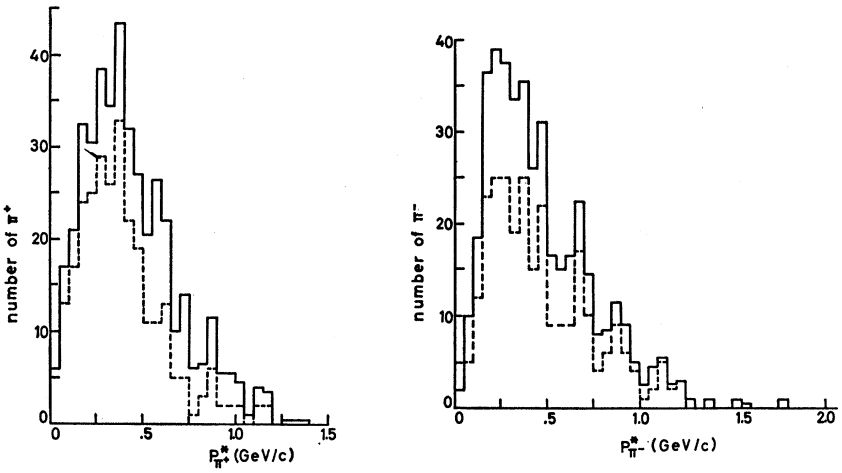

FIG. 10. C.m.-system momentum distributions for reaction $\pi^- p \to n\pi^-\pi^+\pi^-\pi^+(m\pi^0)$; (a) π^+, (b) π^-.

predominantly in the forward direction. The forward peaking in the π^- distributions increases as the number of final-state particles decreases. The π^+ distributions are also peaked forward except for reaction (3b) in which the π^+ are more isotropically distributed. However the π^+ forward peaking, again decreasing with increasing multiplicity, is less than the peaking for π^-. In addition there is generally an accumulation of π^+ in the backward direction, i.e., a depopulation of the angular region about 90°. The π^0 distribution from reaction (2a) is also rather strongly peaked forward. In general one can conclude that the nucleon exhibits a strong tendency to continue in its initial direction while the pions tend to go in the direction of the initial π^-.

It is interesting to compare these results with the angular distributions obtained for the same reactions by the British-German collaboration at 4 GeV/c.[5] At this primary momentum the nucleons show a backward peaking which is however weaker than at 10 GeV/c. Also the π^- forward peaking is much weaker at 4 GeV/c than at 10 GeV/c: At 4 GeV/c for reactions (2b), (3a) and (3b) the π^- distributions are nearly isotropic; at 10 GeV/c the π^- forward peaking remains in all reactions. For reaction (1) 30% of the π^- have $\cos\Theta^* > 0.8$ at 4 GeV/c whereas at 10 GeV/c the corresponding number is 52%. For reaction (2a) the numbers are 18% and 32%, respectively. In contrast to the π^+ distributions at 10 GeV/c, all π^+ distributions at 4 GeV/c are rather isotropic except for reaction (2b) for which the π^+ is slightly peaked forward. Also the π^0 from reaction (2a) is peaked forward more strongly at 10 GeV/c than at 4 GeV/c.

It is worthwhile mentioning that the general features of the angular distributions discussed here (backward peaking of the nucleon, forward peaking of π^-, less forward peaking and some backward accumulation of π^+, flattening out of the distributions with increasing multiplicity) have also been observed in a study of $\pi^- p$ interactions at 16 GeV/c.[6]

The angular distributions of Figs. 1–5 suggest that the reactions (1) to (3b) proceed predominantly via peripheral collisions in which the primary particles keep their original directions. The peripheral nature of the collision seems to become weaker with increasing multiplicity. In agreement with this picture is the fact that the peaking of the angular distributions increases with increasing energy as the comparison of the 4 GeV/c results with the results at 10 GeV/c has shown.

The c.m.-system momentum distributions of the particles involved in the reactions (1) to (3b) are shown in Figs. 6–10. The solid curves represent the invariant phase-space distributions. For reactions (3a) and (3b)

TABLE II. Average transverse momenta.

Channel	Particle	$\bar{p}_\perp$ (MeV/c) 10 GeV/c	4 GeV/c
$p\pi^-\pi^+\pi^-$	p	373±25	407±16
	π^+	330±19	276±11
	π^-	358±16	352±10
$p\pi^-\pi^+\pi^-\pi^0$	p	445±21	398±13
	π^+	327±17	266±10
	π^-	402±14	304±8
	π^0	469±25	294±13
$n\pi^-\pi^+\pi^-\pi^+$	n	528±36	362±17
	π^+	400±18	306±10
	π^-	429±21	289±9
$p\pi^-\pi^+\pi^-(m\pi^0)$	p	394±15	323±18
	π^+	250±12	216±15
	π^-	321±10	233±11
$n\pi^-\pi^+\pi^-\pi^+(m\pi^0)$	π^+	301±9	240±8
	π^-	324±10	254±9
All channels	All nucleons	429±11	385±8
	All pions	348±5	288±3

[5] Aachen-Birmingham-Bonn-Hamburg-London-München collaboration, Nuovo Cimento **21**, 485 (1964).

[6] S. J. Goldsack, L. Riddiford, B. Tallini, B. R. French, W. W. Neale *et al.*, Nuovo Cimento **23**, 941 (1962).

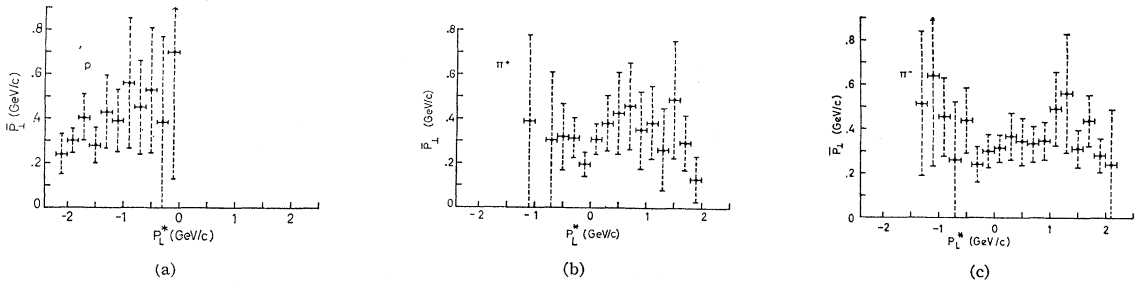

FIG. 11. Average transverse momentum versus c.m.-system longitudinal momentum for reaction $\pi^- p \rightarrow p\pi^-\pi^+\pi^-$; (a) proton, (b) π^+, (c) π^-.

no phase-space curves have been drawn since it is not known how many additional π^0 are produced in these events. One notices strong deviations of the experimental histograms from phase space, especially for the nucleons which tend to have a rather high momentum. The deviations from phase space for the nucleons are again consistent with the peripheral nature of the interaction. If there is a low-momentum transfer to the nucleon then it must generally continue to have a high c.m.-system momentum. The pions, on the other hand (except for the π^0), and in particular the π^+ show a tendency to have low momentum. At 4 GeV/c the same tendency was observed only for reaction (1) whereas for the other reactions the experimental distributions were in good agreement with the phase-space curves.

4. THE TRANSVERSE MOMENTUM

In Table II the average transverse momenta $\bar{p}_\perp$ for the various particles of reactions (1) to (3b) are given. For comparison we also give the corresponding values obtained at 4 GeV/c. The errors have been calculated from the formula

$$\Delta\bar{p}_\perp = [(1/N)(\langle p_\perp^2\rangle_{\rm av} - \langle p_\perp\rangle^2_{\rm av})]^{1/2}, \qquad (4)$$

where N is the number of particles. Thus the ambiguities in the event identification which could affect the values for the nucleons, the π^+ and the π^0, are not taken into account in the errors. At the lower end of the table the values of $\bar{p}_\perp$ obtained for all nucleons and all pions are given for the two primary momenta. It is seen that $\bar{p}_\perp$ is larger for the nucleon than for the pion in agreement with the mass dependence of $\bar{p}_\perp$ observed by Bigi *et al.*[4] Furthermore $\bar{p}_\perp$ increases slightly with increasing primary momentum. Finally, as the table shows, there is also a dependence of $\bar{p}_\perp$ on the charge of the particle and on the multiplicity of the reaction.

Figures 11–15 show the average transverse momentum $\bar{p}_\perp$ as a function of the longitudinal momentum p_L^* in the c.m. system for the particles occurring in the five reactions (1) to (3b). Although such a $\bar{p}_\perp$ versus p_L^* plot

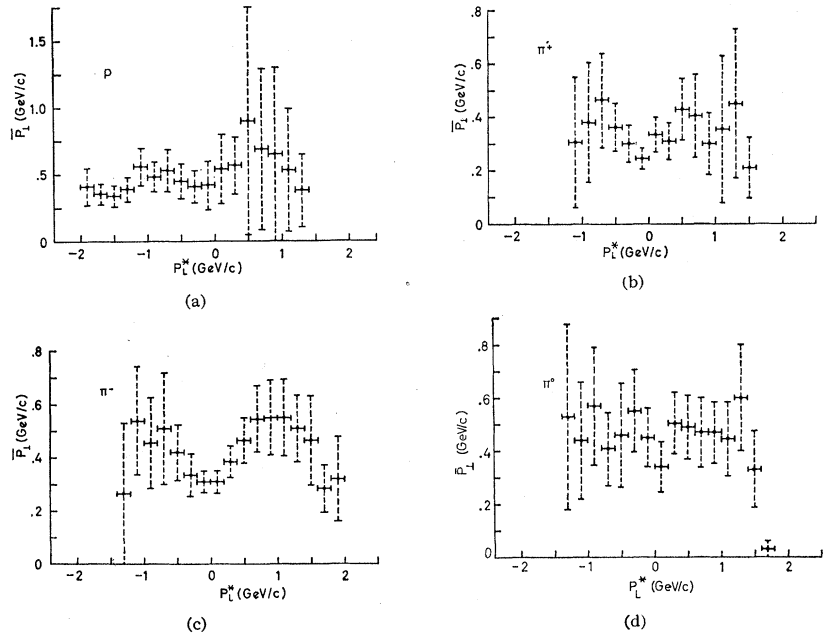

FIG. 12. Average transverse momentum versus c.m.-system longitudinal momentum for reaction $\pi^- p \rightarrow p\pi^-\pi^+\pi^-\pi^0$; (a) proton, (b) π^+, (c) π^-, (d) π^0.

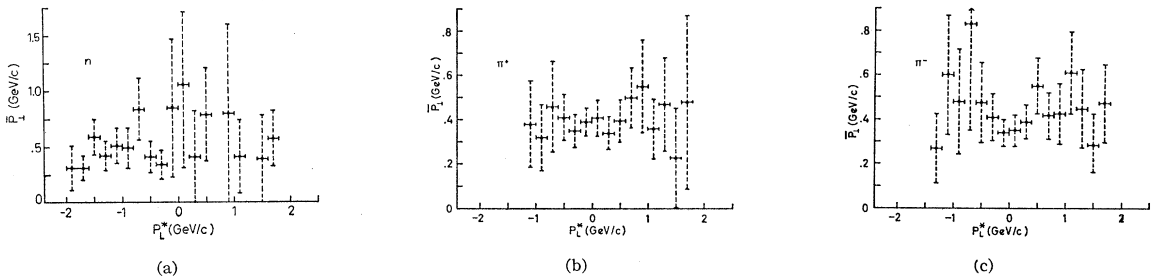

(a) (b) (c)

FIG. 13. Average transverse momentum versus c.m.-system longitudinal momentum for reaction $\pi^- p \to n\pi^-\pi^+\pi^-\pi^+$; (a) neutron, (b) π^+, (c) π^-.

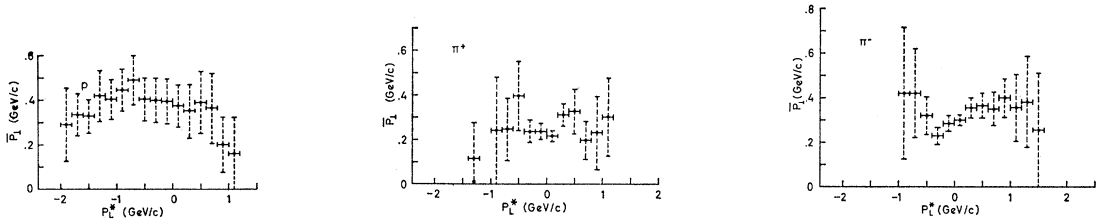

(a) (b) (c)

FIG. 14. Average transverse momentum versus c.m.-system longitudinal momentum for reaction $\pi^- p \to p\pi^-\pi^+\pi^-(m\pi^0)$; (a) proton, (b) π^+, (c) π^-.

FIG. 15. Average transverse momentum versus c.m.-system longitudinal momentum for reaction $\pi^- p \to n\pi^-\pi^+\pi^-\pi^+(m\pi^0)$; (a) π^+, (b) π^-.

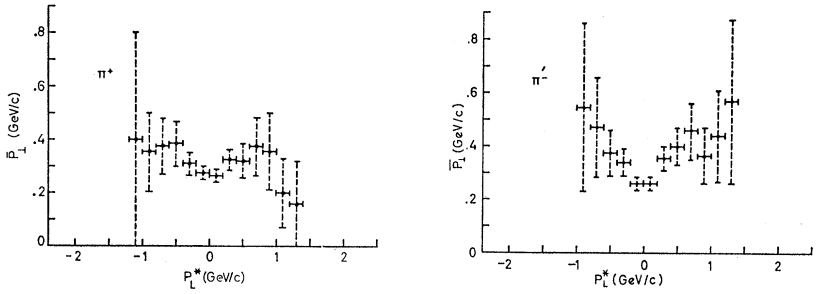

(a) (b)

contains, of course, a little less information than a scatter diagram of $p_\perp$ versus p_L^*, it is quite illustrative for the kinematics of the reaction; it shows immediately the average correlation between scattering angle and momentum since a vector drawn from the origin of the diagram to an experimental point defines a c.m.-system scattering angle by its direction and gives the average momentum for that angle by its length.

The errors assigned to the experimental points in Figs. 11–15 have not been calculated according to formula (4) since in many p_L^* intervals there were only a few particles. We have therefore calculated the "errors" according to $\bar{p}_\perp/\sqrt{N}$. Thus the dotted "error limits" attached to each point in the figures give only an indication of the statistical significance of that point indicating the number of individual $p_\perp$ values from which the point was obtained.

It is seen from the figures that for all particles except the π^- the experimental points seem to fall within statistics more or less on a horizontal straight line; i.e., $\bar{p}_\perp$ seems to be rather independent of the scattering angle. This may not be true for the π^-; the π^- travelling in the c.m. system at about 90° with respect to the primary direction seem to have a lower $\bar{p}_\perp$ than the ones going forward (or backward), at least for the reactions (2a) and (3b). Evidence for $\bar{p}_\perp$ being independent of the scattering angle has been found in the study of high-energy cosmic-ray jets[7]; this constancy of $\bar{p}_\perp$ has been used to determine the energy of jet secondaries from their scattering angles according to $p^* = \text{const}/\sin\Theta^*$.

5. PRODUCTION OF RESONANCES

In order to investigate the occurrence of resonances we have plotted all possible $\pi\pi$ and $N\pi$ effective-mass

[7] B. Edwards, J. Losty, D. H. Perkins, K. Pinkau, and J. Reynolds, Phil. Mag. 3, 237 (1958).

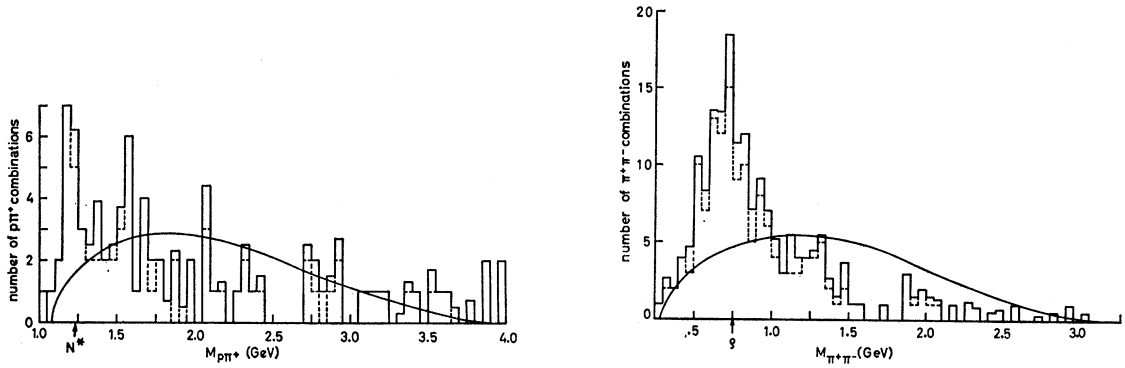

FIG. 16. Effective-mass distributions for reaction $\pi^- p \to p\pi^-\pi^+\pi^-$; (a) $p\pi^+$, (b) $\pi^+\pi^-$.

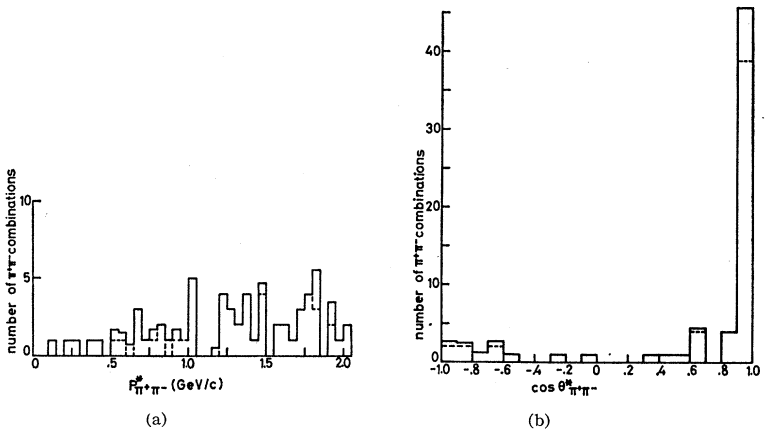

FIG. 17. C.m.-system momentum (a) and angular (b) distribution for the $\pi^+\pi^-$ system in reaction $\pi^- p \to p\pi^-\pi^+\pi^-$ with 0.60 GeV $< M_{\pi^+\pi^-} <$ 0.85 GeV.

distributions for the five reactions (1) to (3b). Whereas at 4 GeV/c these distributions agreed with the invariant phase-space curves rather well except, of course, for the resonance peaks, the agreement at 10 GeV/c was much poorer. In the following only those effective-mass histograms are presented in which a resonance peak has been observed with conclusive evidence (except for Figs. 23b and c). The solid curves represent the invariant phase-space distributions always normalized to the total area under the histograms.

Figure 16 shows the $p\pi^+$ and $\pi^+\pi^-$ effective-mass distribution for reaction (1). It is seen that the N^{*++} and the ρ^0 show up, the latter very strongly. From the number of events in the peaks above the background it has been deduced that about 70% of reaction (1) proceeds via ρ^0 production, about 10% via N^{*++} production and about 20% via the direct channel. In Fig. 17 the c.m.-system momentum and angular distributions for the $\pi^+\pi^-$ systems in the ρ region (0.60 GeV $< M_{\pi^+\pi^-} <$ 0.85 GeV) are plotted. Since about 65% of these $\pi^+\pi^-$ systems are ρ mesons the histograms give an indication of the c.m.-system production momentum and angular distributions for the ρ^0 meson. In particular it is seen that the ρ^0 is produced strongly forward. In Fig. 18 the four-momentum transfer Δ^2 between the $\pi^+\pi^-$ systems in the ρ region and the incident π^- is given. The figure shows that small momentum transfers are preferred which suggests that the one-pion exchange

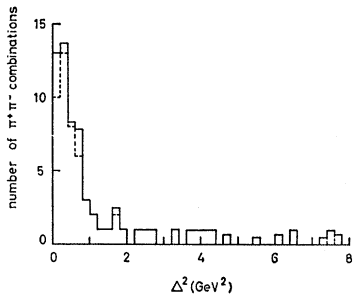

FIG. 18. Δ^2 distribution for the $\pi^+\pi^-$ system in reaction $\pi^- p \to p\pi^-\pi^+\pi^-$ with 0.60 GeV $< M_{\pi^+\pi^-} <$ 0.85 GeV.

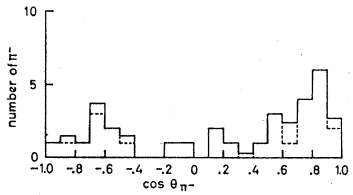

FIG. 19. Distribution of the angle between the incident π^- and the decay π^- in the $\pi^+\pi^-$ rest system for reaction $\pi^- p \to p\pi^-\pi^+\pi^-$, 0.60 GeV $< M_{\pi^+\pi^-} <$ 0.85 GeV and $\Delta^2 <$ 0.6 GeV^2.

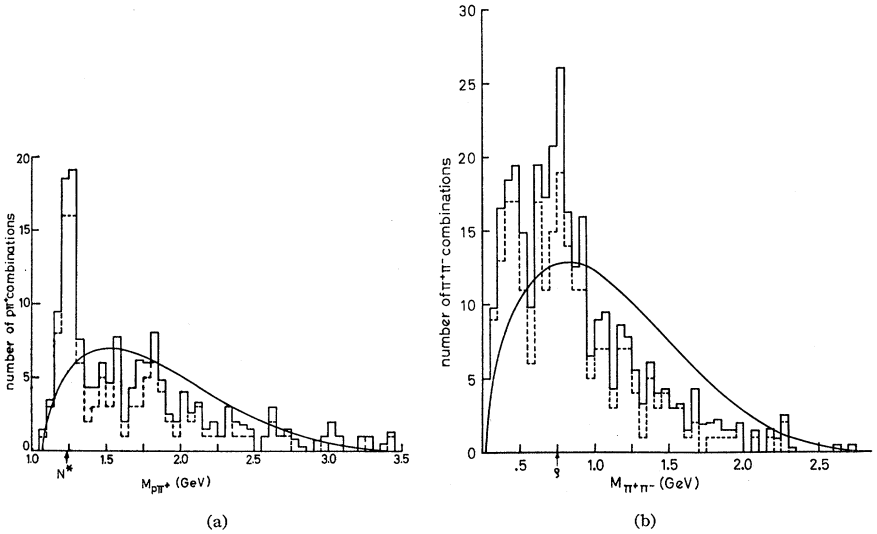

FIG. 20. Effective-mass distributions for reaction $\pi^- p \to p\pi^-\pi^+\pi^-\pi^0$; (a) $p\pi^+$, (b) $\pi^+\pi^-$.

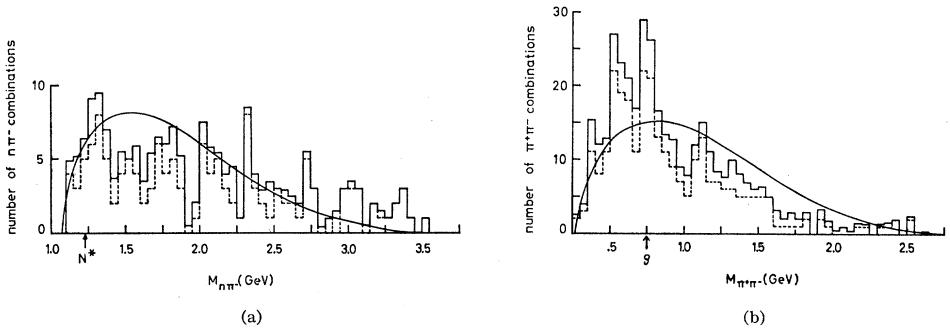

FIG. 21. Effective-mass distributions for reaction $\pi^- p \to n\pi^-\pi^+\pi^-\pi^+$; (a) $n\pi^-$, (b) $\pi^+\pi^-$.

mechanism is important in ρ production. Finally, in order to study the decay of the ρ^0 we have plotted in Fig. 19 the distribution of the decay angle between the π^- from the $\pi^+\pi^-$ combinations in the ρ region and the incident π^- in the $\pi^+\pi^-$ rest system for $\Delta^2 \leqslant 0.6$ GeV^2. One notices the well-known asymmetric decay of the ρ^0 (see, for instance, Refs. 5, 9). From Fig. 19 the asymmetry parameter turns out to be $(F-B)/(F+B) = 0.28 \pm 0.17$.

In Fig. 20 the $p\pi^+$ and $\pi^+\pi^-$ effective-mass distributions for reaction (2a) and in Fig. 21 the $n\pi^-$ and $\pi^+\pi^-$ mass distributions for reaction (2b) are given. The N^{*++} appears quite strongly in reaction (2a) while the N^{*-} peak in reaction (2b) is weaker. For both reactions a peak at the ρ^0 mass is observed in the $\pi^+\pi^-$ mass distribution. There also appear to be $\pi^+\pi^-$ peaks above the background in the neighborhood of 500 MeV for both reactions. These peaks might be associated with a di-pion resonance in this energy region reported by other groups for incident pion energies near 4 GeV.[5,10] Another possibility is that the surplus of events above phase space at low $\pi\pi$ effective masses is a kinematic effect associated with the peripheral nature of the interactions (see discussion of Fig. 23). In Fig. 22 the $\pi^+\pi^-\pi^0$ effective-mass distribution for reaction (2a) is shown; the peak around 780 MeV is due to the ω^0 meson.

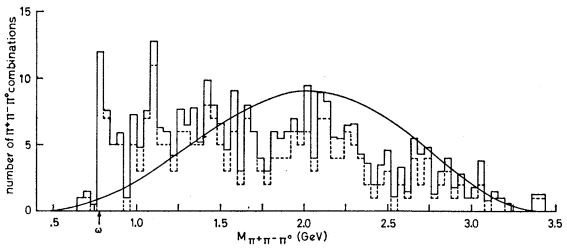

FIG. 22. $\pi^+\pi^-\pi^0$ effective-mass distribution for reaction $\pi^- p \to p\pi^-\pi^+\pi^-\pi^0$.

[8] ICF-collaboration: to be published in Nuovo Cimento.
[9] Aachen-Birmingham-Bonn-Hamburg-London-München collaboration, Phys. Letters **5**, 153 (1963).
[10] N. P. Samios, A. H. Bachman, R. M. Lea, T. E. Kalogeropoulos, and W. D. Shephard, Phys. Rev. Letters **9**, 139 (1962).

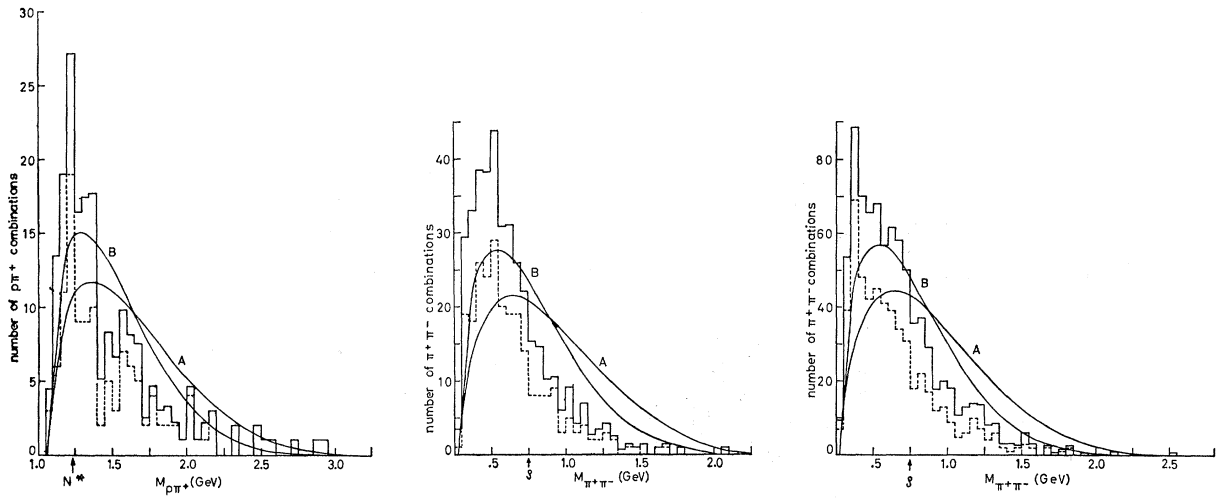

FIG. 23. Effective-mass distributions for reaction $\pi^- p \rightarrow p\pi^-\pi^+\pi^-(m\pi^0)$, (a) $p\pi^+$, (b) $\pi^+\pi^-$, and for reaction $\pi^- p \rightarrow n\pi^-\pi^+\pi^-\pi^+(m\pi^0)$, (c) $\pi^+\pi^-$. The curves represent the phase-space distributions for five (curve A) and six (curve B) secondary pions.

TABLE III. Cross sections for production of resonant states.

Reaction	Cross section (mb)
$\pi^- p \rightarrow N^{*++}\pi^-\pi^-$	0.10±0.04
$\rightarrow p\pi^-\rho^0$	0.70±0.10
$\rightarrow N^{*++}\pi^-\pi^-\pi^0$	0.36±0.08
$\rightarrow p\pi^-\pi^0\rho^0$	0.27±0.12
$\rightarrow N^{*-}\pi^+\pi^-\pi^+$	0.11±0.05
$\rightarrow n\pi^-\pi^+\rho^0$	0.19±0.07
$\rightarrow p\pi^-\omega^0$	0.12±0.05

From the resonance peaks in the Figs. 16, 20–22 cross sections have been deduced for the production of resonances in the various reactions. The cross section values are summarized in Table III.

Some conclusions may be drawn from an examination of the effective-mass distributions for events in categories (3a) and (3b) for which the number of neutral pions is not known. From the relative number of events observed with 6, 8, and 10 charged secondaries[1] it seems probable that the majority of our reactions (3a) and (3b) are events with 5 and 6 secondary pions. In Fig. 23 are shown the $p\pi^+$ effective-mass distribution for events of type (3a) and the $\pi^+\pi^-$ mass distributions for events of types (3a) and (3b) together with the phase-space distributions for final states with 5 (curve A) and 6 (curve B) pions. Each curve is normalized to the total area under the histogram. For each distribution the "true" phase-space curve, depending on the relative frequency of events with 5 and 6 secondary pions, should lie somewhere between the two curves shown.

However one must question the validity of estimating the background by comparison with phase space. For the $\pi\pi$ effective-mass distributions, except perhaps for the $\pi^-\pi^-$ distribution for reaction (3a), there appear to be many more combinations with masses below about 600 MeV than any reasonable background based on the phase-space curves would predict. Deviations from phase-space predictions are also observed in the effective-mass distributions of reactions (1), (2a) and (2b); they are not unexpected in view of the peripheral characteristics exhibited by interactions at this energy. A surplus of low $\pi\pi$ effective masses in comparison with phase space will automatically result if all the pions tend to go forward in the c.m. system. But such a simple picture would not predict the observed surplus of events (3a) with low $p\pi^+$ effective masses. In view of the uncertainties about the detailed nature of the interaction the best estimate of the background might be obtained by drawing smooth curves through those parts of the experimental distributions where no resonances are expected and then extending them smoothly to the whole distributions.

Certain features in the experimental distributions of Fig. 23 are apparent for any reasonable estimate of the background: In the $p\pi^+$ distribution a peak at the N^* mass is clearly present. We can thus conclude that N^{*++} production is significant at this energy even for final states with higher multiplicity. In the $\pi^+\pi^-$ distributions for both (3a) and (3b) events no peaking at the ρ^0 mass is observed. We conclude that ρ^0 production is not significant at this energy for events with higher multiplicity.

ACKNOWLEDGMENTS

We are very much indebted to the staff of the CERN proton synchrotron and to the crews of the 81-cm Saclay hydrogen bubble chamber. Furthermore, we are

very grateful to our scanners for their help in scanning and measuring the events and analyzing the data. We also want to thank many colleagues, specially Dr. L. von Lindern, Dr. D. Lüers and Dr. D. R. O. Morrison for helpful discussions and valuable suggestions. The interest and support of Dr. K. Gottstein in this experiment are greatly appreciated. Finally we thank G. Wolf for the computation of the phase-space curves.

PHYSICAL REVIEW VOLUME 134, NUMBER 4B 25 MAY 1964

Improved Minimum Principle for Multichannel Scattering*

YUKAP HAHN, THOMAS F. O'MALLEY,† AND LARRY SPRUCH
Physics Department, New York University, Washington Square, New York, New York

(Received 13 December 1963)

If the open-channel target states are known, the minimum principle formulation of scattering theory provides a systematic approach whereby one can, to arbitrary precision, monotonically approach the reactance matrix **K**. The scattering wave function and the Green's function for the open-channel approximation, that in which the closed channels are not taken into account at all, must be solved numerically. An explicit method for constructing the Green's function is given. The minimum principle approach is probably limited at present, in practice though not in principle, to the three-body problem with just a few open channels. A very useful simplification is possible at the threshold for a new channel; one need not there include the new channel in the equations that must be solved exactly.

1. INTRODUCTION

THE minimum principle formulation of scattering theory was originally restricted to the case for which the initial relative kinetic energy of the two systems, E', was zero.[1] The formulation was a practical one and was applied to a number of scattering problems.[2] The initial extension[3] to $E'>0$ was not quite in a practical form, but recently an improved (and truly rigorous) formalism was derived[4] for $E'>0$ which can and has been applied to single-channel scattering by a compound system. The present paper will be primarily devoted to extending this newer minimum principle formulation to multichannel scattering. It will be useful to begin with a brief outline of the results that were previously obtained. The notation to be used will be that of Ref. 4 and of a paper on bounds on multichannel scattering parameters.[5] (As opposed to some of the earlier usage, we here distinguish between bounds and minimum principles; minimum principles, which might alternattively be called variational bounds, contain variational parameters, while bounds do not.)

For simplicity, we consider the scattering of a particle by a compound system, rather than of one compound system by another, and we take the incident particle to be distinguishable from the target particles, to have no spin or orbital angular momentum and to have no charge; we further assume that no rearrangement processes are possible, and that the ground state and all of the excited states of the target have zero angular momentum. Under most circumstances these restrictions can be trivially relaxed. We also assume this time not for simplicity but because of a basic limitation of the minimum principle approach, that the incident energy is too small to produce breakup.

Let the target have eigenfunctions $\psi_{Tm}(\mathbf{r})$ and associated energy eigenvalues E_{Tm}, where $m=0, 1, 2, \cdots$, and assume that the total energy E lies between $E_{T,N-1}$ and E_{TN}, so that there are N open channels. It will unfortunately be necessary to assume that the open-channel eigenfunctions and energy eigenvalues are known. This is only natural since the eigenfunctions and eigenvalues appear explicitly in the specification of the boundary conditions. We let the index i refer to open channels, and let k_i and μ_i represent the wave number and the reduced mass in channel i. We now introduce for the moment the trial function Ψ_t which is

* The research reported on in this article was sponsored by the U. S. Army Research Office, Durham, N. C. under Grant No. DA-ARO-(D)-31-124-G276, under Contract No. AF 19(604)4555, Project No. 7635, Task No. 76361, the Office of Naval Research, and the Advanced Research Projects Agency under Contract Nonr-285(49), NR 012-109.

† Presently visiting fellow, Joint Institute for Laboratory Astrophysics, Boulder, Colorado.

[1] L. Spruch and L. Rosenberg, Phys. Rev. **116**, 1034 (1959); **117**, 1095 (1960); L. Rosenberg, L. Spruch, and T. F. O'Malley, *ibid.* **118**, 184 (1960).

[2] The various references are given by L. Spruch, in *Lectures in Theoretical Physics, Boulder, 1961* (Interscience Publishers, Inc., New York, 1961), Vol. 4.

[3] L. Spruch and L. Rosenberg, Phys. Rev. **120**, 474 (1960); L. Rosenberg and L. Spruch, *ibid.* **121**, 1720 (1961); **125**, 1407 (1962).

[4] Y. Hahn, T. F. O'Malley, and L. Spruch, Phys. Rev. **130**, 381 (1963).

[5] Y. Hahn, T. F. O'Malley, and L. Spruch, Phys. Rev. **134**, B397 (1964).